Structural diversity in the RGS domain and its interaction with heterotrimeric G protein α-subunits

Meera Soundararajan*, Francis S. Willard†, Adam J. Kimple†, Andrew P. Turnbull*, Linda J. Ball‡, Guillaume A. Schoch*, Carina Gileadi*, Oleg Y. Fedorov*, Elizabeth F. Dowler‡, Victoria A. Higman‡, Stephanie Q. Hutsell†, Michael Sundström*§, Declan A. Doyle*¶, and David P. Siderovski†‖

*Structural Genomics Consortium, Oxford University, Oxford OX3 7DQ, United Kingdom; †Department of Pharmacology, University of North Carolina, Chapel Hill, NC 27599; and ‡Leibniz-Institut für Molekulare Pharmakologie, Robert-Rössle Strasse 10, 13125 Berlin, Germany

Regulator of G protein signaling (RGS) proteins accelerate GTP hydrolysis by Gα subunits and thus facilitate termination of signaling initiated by G protein-coupled receptors (GPCRs). RGS proteins hold great promise as disease intervention points, given their signature role as negative regulators of GPCRs—receptors to which the largest fraction of approved medications are currently directed. RGS proteins share a hallmark RGS domain that interacts most avidly with Gα when in its transition state for GTP hydrolysis; by binding and stabilizing switch regions I and II of Gα, RGS domain binding consequently accelerates Gα-mediated GTP hydrolysis. The human genome encodes more than three dozen RGS domain-containing proteins with varied Gα substrate specificities. To facilitate their exploitation as drug-discovery targets, we have taken a systematic structural biology approach toward cataloging the structural diversity present among RGS domains and identifying molecular determinants of their differential Gα selectivities. Here, we determined 14 structures derived from NMR and x-ray crystallography of members of the R4, R7, R12, and RZ subfamilies of RGS proteins, including 10 uncomplexed RGS domains and 4 RGS domain/Gα complexes. Heterogeneity observed in the structural architecture of the RGS domain, as well as in engagement of switch III and the all-helical domain of the Gα substrate, suggests that unique structural determinants specific to particular RGS protein/Gα pairings exist and could be used to achieve selective inhibition by small molecules.

GTPase-accelerating proteins | NMR structure | RGS proteins | x-ray crystallography

G protein-coupled receptors (GPCRs) are critical for many physiological processes including vision, olfaction, neurotransmission, and the actions of many hormones (1). As such, GPCRs are the largest fraction of the "druggable proteome," and their ligand-binding and signaling properties remain of considerable interest to academia and industry (2). GPCRs catalyze activation of heterotrimeric G proteins comprising a guanine nucleotide-binding Gα subunit and an obligate Gβγ dimer (3). Receptor–promoted activation of Gαβγ causes exchange of GDP for GTP by Gα and resultant dissociation of Gβγ. GTP-bound Gα and freed Gβγ then regulate intracellular effectors such as adenylyl cyclase, phospholipase C, ion channels, RhoGEFs, and phosphodiesterases (1, 4). This "G protein cycle" is reset by the intrinsic GTP hydrolysis activity of Gα, producing Gα·GDP that favors heterotrimer reformation and, consequently, signal termination. Thus, a major determinant of the duration and magnitude of GPCR signaling is the lifetime of Gα in the GTP-bound state.

Regulators of G protein signaling are GTPase-accelerating proteins (GAPs) for Gα subunits and thus facilitate GPCR signal termination (5). GAP activity is conferred by an RGS domain present in one or more copies within members of this protein superfamily (5). The archetypal RGS domain is composed of nine α-helices (6) and binds most avidly to Gα in the transition state for GTP hydrolysis (7); by stabilizing the flexible switch regions of Gα, RGS domain binding accelerates Gα-mediated GTP hydrolysis. Thirty-seven proteins containing at least one region of homology to the archetypal RGS domain fold are encoded by the human genome (5), broadly classified into eight subfamilies. The R4 (RGS1, -2, -3, -4, -5, -8, -13, -16, -18, -21) and RZ (RGS17, -19, -20) subfamilies generally constitute little more than an RGS domain, although roles for short N-terminal extensions in membrane-targeting and receptor-selective functions have been described (8). The R7 subfamily of RGS6, -7, -9, and -11 form dimers with Gβ5 (9) via a Gγ-like domain N-terminal to their RGS domain. The R12 subfamily constitutes RGS10, -12, and -14, with the latter two sharing additional domains reflecting unique roles as Ras/Raf/MAPK scaffolds (10). The other four subfamilies are signaling regulators that have since become associated with the RGS protein superfamily (5, 11) upon discovery of more distantly related RGS domains within them (i.e., Axin, Axil; RhoGEFs p115-RhoGEF, LARG, and PDZ-RhoGEF; the sorting nexins SNX13, -14, and -25; the GPCR kinases GRK1–7). The RGS domains within the RhoGEF and GPCR kinase subfamilies have also been referred to as rgRGS or RH domains, respectively (12, 13).

RGS proteins control the timing and duration of specific physiological processes that involve GPCR signaling. For example, RGS2-deficient mice exhibit heightened anxiety (14, 15) and constitutive hypertension (16), the latter caused by loss of homeostatic control over vasoconstrictive hormonal signaling via Gq-coupled GPCRs in the vasculature (17). RGS2 is unique among the R4 subfamily in its selectivity for Gαq in vitro (18), although in the context of intact cells or reconstituted receptor/heterotrimer complexes, activity of RGS2 on Gαi-mediated signaling is also seen (19, 20). Differences in Gα selectivity lie, at least in part, in heterogeneity within the structural determinants of Gα engagement by the RGS domain; initial evidence of heterogeneity was seen in the structures of p115-RhoGEF and
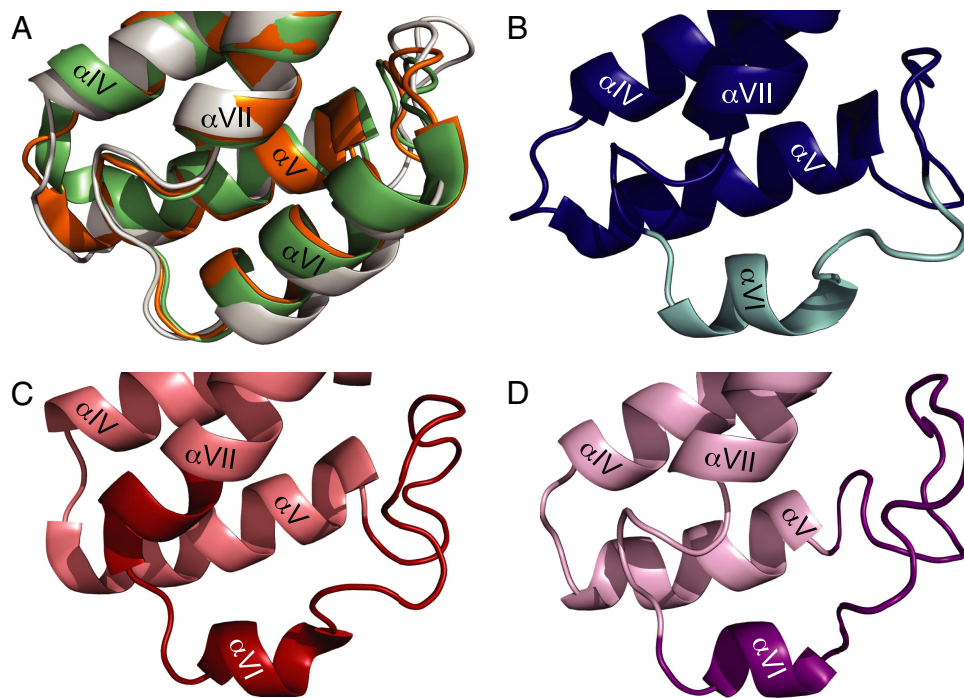
PHARMACOLOGY

Fig. 1. Heterogeneity in the αV–αVII regions of R12 subfamily RGS domains versus the canonical RGS domain fold of R4, R7, and RZ subfamily members. (*A*) Apo-RGS domains of R4 subfamily member RGS8 (green; PDB ID 2IHD), R7 subfamily member RGS9 (orange; PDB ID 1FQI), and RZ subfamily member RGS19 (gray; PDB ID 1CMZ) were aligned along helices αIV and αV and superimposed by using PyMOL. (*B–D*) Apo-RGS domains of RGS14 (*B*) (blue; PDB ID 2JNU), RGS10 from this study (*C*) (salmon; PDB ID 2I59), and RGS10 from Yokoyama *et al.* (*D*) (light purple; PDB ID 2DLR) are presented to highlight differences in the αV–αVI–αVII region. The heterogeneous αVI regions are specifically highlighted in cyan (*B*), red (*C*), and magenta (*D*), respectively.

GRK2 bound to $G\alpha_{13}$ and $G\alpha_q$, respectively (12, 13), that exhibit unique contacts not observed in the first resolved structures [i.e., RGS4/$G\alpha_{i1}$ and RGS9/$G\alpha_t$; (6, 21)]. To assess the structural diversity and $G\alpha$ selectivities of RGS domains, we have taken a systematic structural biology approach and present 14 structures of RGS domains from the R4, RZ, R7, and R12 subfamilies, including four RGS domain/$G\alpha$ complexes, two of which involve $G\alpha_{i3}$. In an accompanying work, Slep *et al.* (22) describe two additional structures of RGS16—uncomplexed and bound to $G\alpha_o$. Detailed knowledge of RGS protein substrate specificity, and the unique structural determinants underlying such specificity, should greatly facilitate exploitation of these GPCR signaling regulators as drug targets (23).

Results and Discussion

Heterogeneity in $G\alpha$ Selectivity and αV–αVII Helical Structures. We purified the RGS domains of 14 human RGS proteins from the R4, RZ, R7, and R12 subfamilies [supporting information (SI) Fig. S1] and assessed their binding to $G\alpha_{i1}$ and $G\alpha_q$ by using surface plasmon resonance spectroscopy (SPR) (Fig. S2 and Table S1). RGS2 was $G\alpha_q$ selective, RGS6, -7, -12, and -14 were $G\alpha_{i1}$ selective, and RGS1, -3, -4, -8, -16, -17, and -18 bound to both $G\alpha_{i1}$ and $G\alpha_q$ (Fig. S2). RGS10 and -20 were $G\alpha_{i1}$ selective, but some binding to $G\alpha_q$ was observed in the specificity screen (Fig. S2). Dose–response studies showed that RGS10 binds with high affinity to $G\alpha_{i1}\cdot GDP\cdot AlF_4^-$ ($K_D \approx 60$ nM) but has much weaker affinity for $G\alpha_q\cdot GDP\cdot AlF_4^-$ ($K_D \geq 3$ μM; Fig. S3). In contrast, RGS20 has weak affinity for both $G\alpha_{i1}\cdot GDP\cdot AlF_4^-$ and $G\alpha_q\cdot GDP\cdot AlF_4^-$ (Fig. S3), consistent with evidence that RGS20 is $G\alpha_z$-selective (24, 25). However, RGS20 also regulates $G\alpha_i$ subunits in cell-expression studies (26).

We determined structures of 10 uncomplexed ("apo") RGS domains from the R4, RZ, R7, and R12 subfamilies by using crystallography and NMR (Table S2). Other structures of apo-RGS domains from these families have also been deposited in the Protein Data Bank (PDB) by others (Table S2 and refs. 21, 22, 27, and 28). Canonical RGS domains consist of a nine-helix bundle comprising two lobes formed by the αI, αII, αIII, αVIII, and αIX helices and the αIV, αV, αVI, and αVII helices, respectively. The majority of apo-RGS domain structures we obtained conform to the structural archetype established by RGS4 (6, 28). Crystal structures of RGS6 and RGS7 (PDB IDs 2ES0 and 2A72) are atypical, domain-swapped dimers. The significance of such dimerization is not known and likely arises because of crystal packing-induced interactions; an NMR solution structure of RGS7 (PDB ID 2D9J) conforms to the canonical RGS domain structure.

Substantial differences were observed between the R12 subfamily RGS domain structures and the prototypical RGS domains of R4, R7, and RZ subfamily members (Fig. 1). NMR structures of RGS10 and RGS14 reveal an extended αV–αVI loop compared with representative members of the R4, R7, and RZ families (Fig. 1 and Fig. S4*A*). The αV–αVI loop of canonical RGS domains is typically 14 residues; this is extended up to 18 residues in RGS10 and RGS14 (Fig. S4*A*). The αVI helical region is also dramatically altered in RGS10 and RGS14 (Fig. 1). RGS10 and RGS14 do not have complete αVI helices *per se* but extended loops with pseudohelical conformations. In our RGS10 solution structure (PDB ID 2I59), the region Leu-90 to Glu-108 (Fig. S4*A*) shows high flexibility as reflected by low ^{15}N-^1H nuclear Overhauser effect (NOE) values (0.5–0.6) and a reduced T1/T2 ratio compared with well ordered parts of the structure (data not shown). The αVII helix of RGS10 also begins one full turn earlier than that of canonical RGS domains (Fig. 1*A* vs. 1*C*). RGS14 displays a similar conformation to RGS10 in the αV–αVI region (Fig. 1*B*), with the exception that the αVII helix begins in its normal position (Fig. 1*A* vs. 1*B*). An alternative NMR structure of RGS10 (PDB ID 2DLR) exhibits a structure nearer that of RGS14 (Fig. 1*D* and Fig. S7*A*).
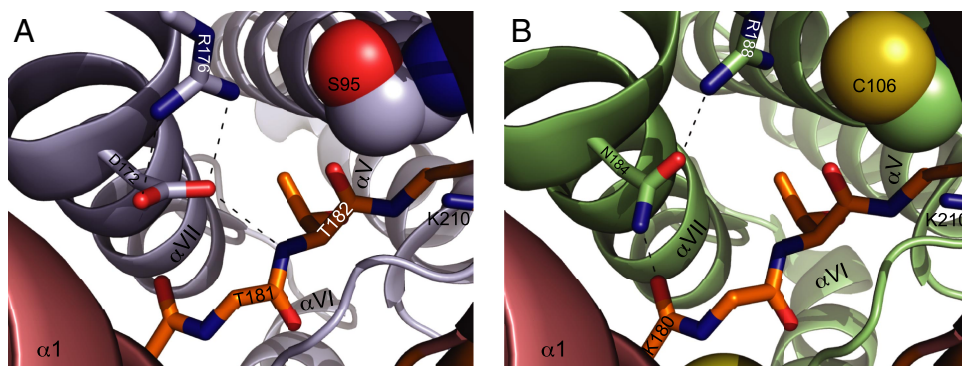
Fig. 2. Predicted structural determinants of Gα selectivity by RGS2. (*A*) RGS1 (gray-blue) bound to Gα$_{i1}$ (α1 helix in light red; switch I in orange) is presented to highlight the Gα switch-I interaction interface (PDB ID 2GTP). Asp-172 of RGS1 is within hydrogen-bonding distance of the backbone amine of Thr-182 in Gα$_{i1}$ and additionally stabilized by the terminal amines of the highly conserved Arg-176 in the RGS1 αVII helix. Ser-95 is placed within close proximity (≤4.0 Å) of three Gα$_{i1}$ residues (Thr-182, Gly-183, and Lys-210). (*B*) Residues 170–190 of RGS2 (PDB ID 2AF0) were superimposed on residues 159–179 of RGS1 from the RGS1/Gα$_{i1}$ complex (PDB ID 2GTP) with an r.m.s.d. of 0.5 Å. RGS1 is not shown, RGS2 is presented in green, and Gα$_{i1}$ is rendered in light red (α1 helix) and orange (switch I). Asparagine at position 184 in RGS2 (normally an aspartate in R4 subfamily members) does not allow for the hydrogen bond to the peptide bond amine of Thr-182 in Gα$_{i1}$; however, Asn-184 can potentially form a hydrogen bond with the backbone carbonyl of Lys-180. The increased atomic radius of Cys-106 in RGS2 (versus serine in RGS1) may cause steric hindrance with the switch-I backbone and the side-chain of Lys-210.

Predicted Basis for Gα$_q$ Selectivity by RGS2. RGS2 is unique in interacting selectively with Gα$_q$ but not Gα$_i$ proteins *in vitro*$^∥$ (Table S1 and ref. 18). Comparing apo-RGS2 (PBD ID 2AF0) with structures of R4-subfamily RGS proteins complexed with Gα$_{i1}$ highlights potential structural determinants preventing RGS2 from interacting with Gα$_i$ *in vitro*. In RGS2, an Asp-to-Asn substitution has occurred at residue 184—a position highly conserved among the R4 subfamily (Fig. S5*A*). Similar to the RGS4/Gα$_{i1}$ and RGS16/Gα$_o$ complexes (6, 22), the aspartate in this position (Asp-172) in our RGS1/Gα$_{i1}$ complex (PDB ID 2GTP) functions as a hydrogen bond acceptor with both the main-chain NH of the Gα$_{i1}$ switch-I residue Thr-182 and the side chain from Arg-176 of RGS1 (Fig. 2*A*). The ε-NH group of Arg-176, in turn, forms a hydrogen bond with Glu-93 of RGS1, stabilizing the C-terminal portion of the αIII helix. Superimposing RGS2 onto the RGS1/Gα$_{i1}$ complex (Fig. 2*B*), the intermolecular hydrogen bond (seen in RGS1 between the δ-oxygen of Asp-172 and the backbone amine of Thr-182) would be lost to RGS2. Mutagenic studies have implicated Asn-184 as being critical to RGS2 Gα selectivity (29). However, in these studies, two other conserved residues (Cys-106 and Glu-191) were also mutated to the corresponding RGS4 residues, Ser and Lys, respectively. Although Ser-95 of RGS1 does not make any critical contacts with Gα$_{i1}$, atoms from Gα$_{i1}$ residues Thr-182, Gly-183, and Lys-210 are all <4.0 Å away from Ser-95 of RGS1. Thus, the presence of cysteine at this position within RGS2 may sterically clash with one or more of these three Gα$_{i1}$ residues (Fig. 2*B*). A double point mutant of RGS2, Cys-106 to serine and Asn-184 to aspartate, does show binding affinity for Gα$_{i1}$ above that of wild-type RGS2 (Fig. S5*B*). The final amino acid determined to be important in RGS2 selectivity for Gα$_q$ is Glu-191, which is a lysine in both RGS1 (Lys-179) and RGS4 (ref. 29). Although the terminal amine of the Lys-179 residue of RGS1 is disordered in the RGS1/Gα$_{i1}$ complex structure, this Lys-179 is directed toward the αA helix of Gα$_{i1}$, and swapping the charge at this position (i.e., Glu-191 of RGS2) may result in a repulsive interaction with αA residues of Gα$_{i1}$.

$^∥$Ingi *et al.* (19) and Cladman and Chidiac (20) have shown that, in a membrane reconstitution system with GPCR and Gα$βγ$ heterotrimer present, RGS2 can serve as an efficient GAP for Gα$_i$ subunits. The reason for the discrepancy between solution-based and membrane-based assays of Gα selectivity is as yet unresolved, but it is of note that RGS2 has multiple GAP-independent effects on GPCR function and signal transduction (42).

Heterogeneity in Gα$_i$ Interactions. We also determined structures of four RGS protein/Gα·GDP·AlF$_4^−$ complexes (RGS1/Gα$_{i1}$, RGS16/Gα$_{i1}$, RGS8/Gα$_{i3}$, and RGS10/Gα$_{i3}$; Table S3). All four complexes represent functional pairings as seen in single-turnover GAP assays (Fig. S6). Before our studies, structures of four RGS protein/Gα complexes had been determined: canonical complexes of RGS4/Gα$_{i1}$ and RGS9/Gα$_{t/i1}$ (6, 21), as well as the atypical RGS domain/Gα pairings of p115-RhoGEF/Gα$_{13/i1}$ and GRK2/Gα$_q$ (12, 13).

Apo- vs. Gα-bound RGS domain structures. Comparing apo-RGS1, apo-RGS8, and apo-RGS16 structures with cognate Gα-bound conformations, only minor structural changes are seen in the RGS domains (backbone r.m.s.d. of 0.4, 0.4, and 0.5 Å, respectively; Fig. S7), mainly in their interhelix loops. This is in contrast to a report of appreciable differences (1.9-Å backbone r.m.s.d) between apo-RGS4 and RGS4/Gα$_{i1}$ structures (28). The αVII helix of apo-RGS4 is broken into two distinct helices in the RGS4/Gα$_{i1}$ complex (6), and, consequently, the αI helix (which forms a significant interface with the αVII helix) also has an altered conformation (28). The resultant effect is a slight modification to the switch II-interacting pocket of RGS4. The importance of this particular conformational change upon Gα binding appears to be protein-specific, because it is not shared with RGS1, RGS8, or RGS16 (Fig. S7). Such subtle differences observed in RGS4 conformation may be due to an inherent experimental difference between NMR and crystallography (30). It is notable that the apo-RGS domain crystal structures of R4 subfamily members are highly ordered in their Gα-binding regions, indicative of fairly rigid conformation in these regions.

Gα$_{i1}$ structures. Overall architecture and specific Gα interaction interfaces of the RGS1/Gα$_{i1}$ and RGS16/Gα$_{i1}$ complexes (Fig. S8) are consistent with the archetypal structure of RGS4/Gα$_{i1}$ (backbone r.m.s.d. of 0.54 Å and 0.61 Å, respectively). The interface is highly comparable with the other R4/Gα and R7/Gα complexes, with interaction being via the Gα switch regions and the base of the dual-lobe RGS domain incorporating the αV–αVI loop. The RGS1/Gα$_{i1}$ and RGS16/Gα$_{i1}$ structures highlight the role of the αIII–αIV loop interacting with switch I and switch II of Gα$_{i1}$ as well as the C-terminal region of the αV–αVI loop and the αVI helix interacting with all three switch regions of Gα. Conserved contacts were observed between the αVII helix, αVIII helix, and transition region between these helices with switch I of Gα$_{i1}$, as seen in RGS4/Gα$_{i1}$ and RGS9/Gα$_{t/i1}$ (6, 21). In addition to these conserved contacts with the Gα Ras-like
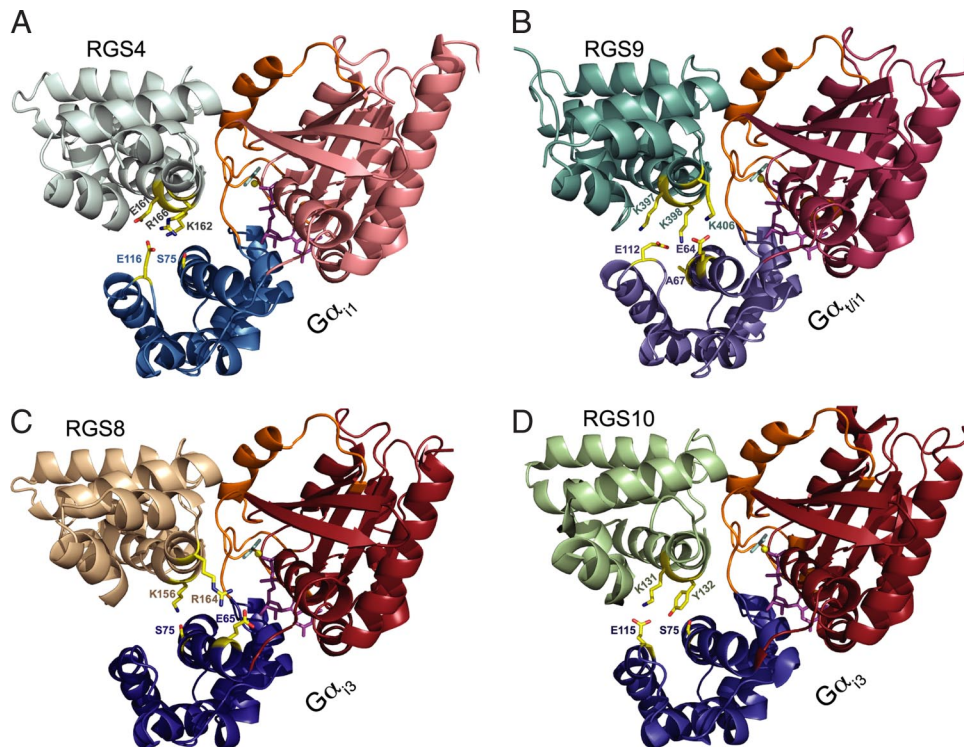
Fig. 3. Heterogeneity in RGS-domain interactions with the Gα all-helical domain. All RGS domain/Gα complexes were aligned and superimposed on the RGS1/Gα$_{i1}$ structure (PDB ID 2GTP) by using PyMOL. The Gα Ras-like domain is colored in shades of red, the all-helical domain is colored in shades of blue, and switch regions are highlighted in orange. GDP, Mg^{2+}, and AlF$_4^-$ are shown in magenta, yellow, and cyan, respectively. All RGS domain residues within 4.0 Å of residues from the Gα all-helical domain are in yellow sticks. (*A*) RGS4/Gα$_{i1}$ complex (PDB ID 1AGR). Glu-161, Lys-162, and Arg-166 in the RGS4 αVII helix are within 4.0 Å of the Gα$_{i1}$ all-helical domain residues Ser-75 or Glu-116. (*B*) RGS9/Gα$_{t/i1}$ complex (PDB ID 1FQK). Three lysine residues in the RGS9 αVII helix at positions 397, 398, and 406 are all within 4.0 Å of Glu-64, Ala-67, and Glu-112 of the Gα$_{t/i1}$ all-helical domain. (*C*) RGS8/Gα$_{i3}$ complex (PDB ID 2ODE). The αVII helix residues Lys-156 and Arg-164 interact with Glu-65 and Ser-75 within the αA helix of the Gα$_{i3}$ all-helical domain. (*D*) RGS10/Gα$_{i3}$ complex (PDB ID 2IHB). Residues Lys-131 and Tyr-132 within the RGS10 αVII helix are within 4.0 Å of Ser-75 and Glu-115 of the Gα$_{i3}$ all-helical domain.

domain, several nonswitch region contacts were observed involving the αV helix, the C terminus of the αVII helix, the αVII–αVIII loop, and the αVIII helix in the RGS1/Gα$_{i1}$ and RGS16/Gα$_{i1}$ complexes, as seen in RGS9/Gα$_{t/i1}$ (21).

Gα$_{i3}$ structures. Our RGS8/Gα$_{i3}$ complex represents a structural view of a Gα$_i$ family member other than Gα$_{i1}$ or transducin. The majority of contacts between RGS8 and Gα$_{i3}$ are made by the switch regions of the Gα$_{i3}$ Ras-like domain and the αIII–αIV loop, αV–αVI loop, and αVII-to-αVIII transition region of RGS8. In addition to these canonical switch region contacts, two contacts were observed between the αVIII helix of RGS8 and the αA helix of the all-helical domain of Gα$_{i3}$. The nature of Gα helical domain contacts will be discussed below.

The Gα$_{i1}$ and Gα$_{i3}$ structures (PDB IDs 2IK8 and 2ODE) are all but identical in overall backbone conformation (0.4 Å r.m.s.d.). All side-chain differences are away from the main face of Gα (i.e., the Gβγ- and effector-binding face), with most differences in the all-helical domain (Fig. S6). The majority of significant (nonconservative) substitutions are on the rear side of the all-helical domain (Fig. S9), suggesting a possible molecular-interaction surface for membrane-delimited GPCR loops and ion-channel domains that might explain the differential biological functions of Gα$_{i1}$ and Gα$_{i3}$ (31–33).

We also determined the structure of the RGS10/Gα$_{i3}$ complex. Consistent with its membership in the R12 subfamily (5), RGS10 is highly selective for Gα$_{i1}$ over Gα$_q$ (Table S1 and Figs. S2 and S3), as are the other R12 subfamily members, RGS12 and RGS14 (34, 35). Gα$_{i3}$ binding by RGS10 is analogous to the R4 subfamily/Gα complexes, involving similar binding motifs such as the conserved RGS domain interaction with Gα switch I

centered about Thr-182. However, comparing RGS10 in its unbound versus Gα$_{i3}$-bound forms (Fig. S7*E*) shows various structural differences that occur upon Gα binding. Apo-RGS10 has a flexible conformation and a small αVI helix (Fig. 1*C* and Fig. S4*A*). Eleven amino acids within RGS10, including αVI, are disordered in the Gα$_{i3}$-bound complex (Fig. S4*A*). Specific interactions between Gα$_{i3}$ and RGS10 within the αV–αVI–αVII region involve Gα$_{i3}$ residues from both switch I and switch II, analogous to R4 subfamily/Gα$_i$ structures (including the following Gα$_{i3}$ residues [with interacting residues(s) from RGS10 in square brackets]: V179 [Y132, D133], K180 [L129, N133], T181 [N133], T182 [S56, L129], G183 [E59, F55], I184 [F55, R137], S206 [Q97], K209 [Q97], and H213 [F55]); however, RGS10 does not retain the typical interactions between switch III and the αVI helix (described below).

Differential switch III interactions. Interaction between a conserved Arg in the αVI helix of the RGS domain (Arg-134 in RGS4) and a highly conserved Glu in switch III of Gα (Glu-236 in Gα$_{i1}$) is seen in all four R4 subfamily complexes determined (RGS1/Gα$_{i1}$, RGS4/Gα$_{i1}$, RGS8/Gα$_{i3}$, and RGS16/Gα$_{i1}$) (Fig. S4*B* and ref. 6). In the RGS9/Gα$_{t/i1}$ structure, this Arg is substituted with Met and the loss of interaction with Glu-236 is compensated by an interaction between this Met and Val-231 of Gα$_t$ (21). In RGS10, this Arg residue is conserved (Arg-105); however, the interaction with switch III of Gα$_{i3}$ is lost (Fig. S4*C*) because the entire αVI helix of RGS10 is disordered in the complex. Arg-105 has a unique conformation in both apo-RGS10 structures, rotated 180° away from the orientation it has in other apo- and Gα-complexed R4-subfamily RGS proteins, as part of helix αVI (Fig. S4). The only switch III interaction observed in the

Soundararajan *et al*.

RGS10/Gα_{i3} complex occurs between the backbone carbonyl of Ala-235[Gα_{i3}] and the backbone amine of Gly-102[RGS10]. Differential capacities for Gα switch III interactions among the R4-, R7-, and R12-subfamily RGS domains could provide a possible mechanism for the Gα_i vs. Gα_q selectivity exhibited by the latter two classes of RGS proteins.

All-helical domain interactions. When comparing RGS4/Gα_{i1} and RGS9/G$\alpha_{t/i1}$ complexes with our structures of RGS8 and RGS10 complexed to Gα_{i3}, there is remarkable heterogeneity in contacts between the αVII and αVIII helices of RGS domains and the Gα all-helical domain. In the RGS4/Gα_{i1} complex, Ser-75 and Glu-116 in Gα_{i1} are within bonding distance (≤ 4.0 Å) of Glu-161, Lys-162, and Arg-166 of RGS4 (Fig. 3*A*). Unlike the switch regions of the G$\alpha_{t/i1}$ chimera (composed of both Gα_t and Gα_{i1} amino acids), the all-helical domain of G$\alpha_{t/i1}$ is composed entirely of Gα_t residues and makes multiple contacts with the αVII and αVIII helices of RGS9 (21). Specifically, Glu-64, Ala-67, and Glu-112 of Gα_t are within 4.0 Å of the RGS9 residues Lys-397, Lys-398, and Lys-406, respectively (Fig. 3*B*). The RGS8/Gα_{i3} complex shows contacts between the RGS8 αVIII helix residues Lys-156 and Arg-164 and the Gα_{i3} αA helix residues Glu-65 and Ser-75 (Fig. 3*C*). Unlike the RGS4/Gα_{i1} and RGS9/G$\alpha_{t/i1}$ structures, no contacts were observed with residues near the αB helix of the Gα_{i3} all-helical domain. Contacts between the RGS10 αVII helix residues Lys-131 and Tyr-132 and the Gα_{i3} all-helical domain residues Glu-115 and Ser-75 are a further example of the all-helical domain serving as an interface for the αVII helix of RGS domains. Yet no contacts whatsoever are apparent between the Gα_{i1} all-helical domain and the RGS domains of RGS1 and RGS16 ([Fig. S8](#)).

The biochemical importance of all-helical domain contacts with the RGS domain in engendering Gα selectivity has been demonstrated for the RGS9/transducin interaction (36). Here, we have shown different RGS proteins (e.g., RGS8, RGS10) recognizing distinct residues within the all-helical domain of the same Gα subunit (e.g., Gα_{i3}; Fig. 3*C* vs. 3*D*). The heterogeneous, but definitive, nature of these contacts suggests that they are likely important in determining *in vivo* Gα selectivity and potency of RGS domain GAP activity. Although the highly conserved interactions with the Gα switch regions may be difficult to target selectively by using chemical biology, perhaps these diverse RGS domain/all-helical domain interactions will be better suited for selective inhibition of specific RGS protein/Gα pairs.

Materials and Methods

Protein Purification and Structure Determinations. Detailed methods are provided in *SI Methods* and Table S4. Purified RGS domains from RGS4 and RGS12, as well as biotinylated Gα_{i1}, were produced as described (37–39).

Surface Plasmon Resonance (SPR) Assays. Surface immobilization of Gα_{i1}-biotin was performed as described (39). The chimeric His$_6$-G$\alpha_{i/q}$ (Gα_q with a 28 amino acid, N-terminal leader from Gα_{i1}) was produced as in ref. 40 and immobilized by using the capture-coupling method exactly as described (41); we refer to this protein as His$_6$-Gα_q throughout. All SPR binding experiments were conducted by using a Biacore 3000 biosensor (GE Healthcare) after equilibrating the sensor surfaces, pump, and fluidic systems with 10 mM Hepes (pH 7.4), 150 mM NaCl, 6 mM MgCl$_2$, 0.05% (vol/vol) Nonidet P-40, and either GDP (100 μM) or GDP·AlF$_4^-$ (100 μM GDP, 20 mM NaF, 30 μM AlCl$_3$).

GAP Assays. RGS protein-mediated acceleration of intrinsic GTP hydrolysis by Gα_{i1} and Gα_{i3} was determined by using single-turnover GTPase assays exactly as described (37).

1. Wettschureck N, Offermanns S (2005) Mammalian G proteins and their cell type specific functions. *Physiol Rev* 85:1159–1204.
2. Jacoby E, Bouhelal R, Gerspacher M, Seuwen K (2006) The 7 TM G protein-coupled receptor target family. *ChemMedChem* 1:761–782.
3. Johnston CA, Siderovski DP (2007) Receptor-mediated activation of heterotrimeric G-proteins: Current structural insights. *Mol Pharmacol* 72:219–230.
4. McCudden CR, Hains MD, Kimple RJ, Siderovski DP, Willard FS (2005) G-protein signaling: Back to the future. *Cell Mol Life Sci* 62:551–577.
5. Siderovski DP, Willard FS (2005) The GAPs, GEFs, and GDIs of heterotrimeric G-protein alpha subunits. *Int J Biol Sci* 1:51–66.
6. Tesmer JJ, Berman DM, Gilman AG, Sprang SR (1997) Structure of RGS4 bound to AlF4-activated G(i alpha1): Stabilization of the transition state for GTP hydrolysis. *Cell* 89:251–261.
7. Popov S, Yu K, Kozasa T, Wilkie TM (1997) The regulators of G protein signaling (RGS) domains of RGS4, RGS10, and GAIP retain GTPase activating protein activity *in vitro*. *Proc Natl Acad Sci USA* 94:7216–7220.
8. Zeng W, et al. (1998) The N-terminal domain of RGS4 confers receptor-selective inhibition of G protein signaling. *J Biol Chem* 273:34687–34690.
9. Snow BE, et al. (1998) A G protein γ-subunit-like domain shared between RGS11 and other RGS proteins specifies binding to Gβ5 subunits. *Proc Natl Acad Sci USA* 95:13307–13312.
10. Willard MD, et al. (2007) Selective role for RGS12 as a Ras/Raf/MEK scaffold in nerve growth factor-mediated differentiation. *EMBO J* 26:2029–2040.
11. Siderovski DP, Hessel A, Chung S, Mak TW, Tyers M (1996) A new family of regulators of G-protein-coupled receptors. *Curr Biol* 6:211–212.
12. Chen Z, Singer WD, Sternweis PC, Sprang SR (2005) Structure of the p115RhoGEF rgRGS domain-Galpha13/i1 chimera complex suggests convergent evolution of a GTPase activator. *Nat Struct Mol Biol* 12:191–197.
13. Tesmer VM, Kawano T, Shankaranarayanan A, Kozasa T, Tesmer JJ (2005) Snapshot of activated G proteins at the membrane: the Galphaq-GRK2-Gbetagamma complex. *Science* 310:1686–1690.
14. Oliveira-Dos-Santos AJ, et al. (2000) Regulation of T cell activation, anxiety, and male aggression by RGS2. *Proc Natl Acad Sci USA* 97:12272–12277.
15. Yalcin B, et al. (2004) Genetic dissection of a behavioral quantitative trait locus shows that Rgs2 modulates anxiety in mice. *Nat Genet* 36:1197–1202.
16. Tang KM, et al. (2003) Regulator of G-protein signaling-2 mediates vascular smooth muscle relaxation and blood pressure. *Nat Med* 9:1506–1512.
17. Heximer SP, et al. (2003) Hypertension and prolonged vasoconstrictor signaling in RGS2-deficient mice. *J Clin Invest* 111:445–452.
18. Heximer SP, Watson N, Linder ME, Blumer KJ, Hepler JR (1997) RGS2/G0S8 is a selective inhibitor of Gqα function. *Proc Natl Acad Sci USA* 94:14389–14393.
19. Ingi T, et al. (1998) Dynamic regulation of RGS2 suggests a novel mechanism in G-protein signaling and neuronal plasticity. *J Neurosci* 18:7178–7188.
20. Cladman W, Chidiac P (2002) Characterization and comparison of RGS2 and RGS4 as GTPase-activating proteins for m2 muscarinic receptor-stimulated G(i). *Mol Pharmacol* 62:654–659.
21. Slep KC, et al. (2001) Structural determinants for regulation of phosphodiesterase by a G protein at 2.0 A. *Nature* 409:1071–1077.
22. Slep KC, et al. (2008) Molecular architecture of G-α-o and the structural basis for RGS16-mediated deactivation. *Proc Natl Acad Sci USA* 105:6243–6248.
23. Neubig RR, Siderovski DP (2002) Regulators of G-protein signalling as new central nervous system drug targets. *Nat Rev Drug Discov* 1:187–197.
24. Glick JL, Meigs TE, Miron A, Casey PJ (1998) RGSZ1, a Gz-selective regulator of G protein signaling whose action is sensitive to the phosphorylation state of Gzalpha. *J Biol Chem* 273:26008–26013.
25. Wang J, et al. (1998) RGSZ1, a Gz-selective RGS protein in brain. Structure, membrane association, regulation by Galphaz phosphorylation, and relationship to a Gz gtpase-activating protein subfamily. *J Biol Chem* 273:26014–26025.
26. Wang Y, et al. (2002) Regulator of G protein signaling Z1 (RGSZ1) interacts with Galpha i subunits and regulates Galpha i-mediated cell signaling. *J Biol Chem* 277:48325–48332.
27. de Alba E, De Vries L, Farquhar MG, Tjandra N (1999) Solution structure of human GAIP (Galpha interacting protein): A regulator of G protein signaling. *J Mol Biol* 291:927–939.
28. Moy FJ, et al. (2000) NMR structure of free RGS4 reveals an induced conformational change upon binding Galpha. *Biochemistry* 39:7063–7073.
29. Heximer SP, et al. (1999) G protein selectivity is a determinant of RGS2 function. *J Biol Chem* 274:34253–34259.
30. Andrec M, et al. (2007) A large data set comparison of protein structures determined by crystallography and NMR: Statistical test for structural differences and the effect of crystal packing. *Proteins* 69:449–465.
31. Ivanina T, et al. (2004) Galphai1 and Galphai3 differentially interact with, and regulate, the G protein-activated K$^+$ channel. *J Biol Chem* 279:17260–17268.

PHARMACOLOGY

32. Rubinstein M, Peleg S, Berlin S, Brass D, Dascal N (2007) Galphai3 primes the G protein-activated K$^+$ channels for activation by coexpressed Gbetagamma in intact *Xenopus* oocytes. *J Physiol* 581:17–32.

33. O'Hara CM, Tang L, Taussig R, Todd RD, O'Malley KL (1996) Dopamine D2L receptor couples to G alpha i2 and G alpha i3 but not G alpha i1, leading to the inhibition of adenylate cyclase in transfected cell lines. *J Pharmacol Exp Ther* 278:354–360.

34. Snow BE, *et al.* (1998) GTPase activating specificity of RGS12 and binding specificity of an alternatively spliced PDZ (PSD-95/Dlg/ZO-1) domain. *J Biol Chem* 273:17749–17755.

35. Cho H, Kozasa T, Takekoshi K, De Gunzburg J, Kehrl JH (2000) RGS14, a GTPase-activating protein for Gialpha, attenuates Gialpha- and G13alpha-mediated signaling pathways. *Mol Pharmacol* 58:569–576.

36. Skiba NP, Yang CS, Huang T, Bae H, Hamm HE (1999) The alpha-helical domain of Galphat determines specific interaction with regulator of G protein signaling 9. *J Biol Chem* 274:8770–8778.

37. Johnston CA, *et al.* (2006) Minimal determinants for binding activated G alpha from the structure of a G alpha(i1)-peptide dimer. *Biochemistry* 45:11390–11400.

38. Kimple AJ, *et al.* (2007) The RGS protein inhibitor CCG-4986 is a covalent modifier of the RGS4 Galpha-interaction face. *Biochim Biophys Acta* 1774:1213–1220.

39. Willard FS, Low AB, McCudden CR, Siderovski DP (2007) Differential G-alpha interaction capacities of the GoLoco motifs in Rap GTPase activating proteins. *Cell Signal* 19:428–438.

40. Rojas RJ, *et al.* (2007) G{alpha}q directly activates p63RhoGEF and Trio via a conserved extension of the Dbl homology-associated pleckstrin homology domain. *J Biol Chem* 282:29201–29210.

41. Willard FS, Siderovski DP (2006) Covalent immobilization of histidine-tagged proteins for surface plasmon resonance. *Anal Biochem* 353:147–149.

42. Heximer SP, Blumer KJ (2007) RGS proteins: Swiss army knives in seven-transmembrane domain receptor signaling networks. Sci STKE 2007, pe2.

Soundararajan *et al.*